Supporting information

Rational Design of NIR Fluorescent Probe for Carboxylesterase 1 Detection During Endoplasmic Reticulum Stress and Drug-Induced Acute Liver Injury

Chaoyan Han [a, b ‡], Xin Zhao [c, ‡], Xiaokui Huo [a], Zhenlong Yu [b], Chao Wang [b], Lei Feng [a, d, e *], Jingnan Cui [c], Xiangge Tian [a *], Xiaochi Ma [a, f *]

[a] Second Affiliated Hospital, Dalian Medical University, Dalian 116023, China.

[b] College of Pharmacy, Dalian Medical University, Dalian 116044, China.

[c] State Key Laboratory of Fine Chemicals, Dalian University of Technology, Dalian 116024, China.

[d] School of Chemistry and Chemical Engineering, Henan Normal University, Xinxiang 453007, China.

[e] Key Laboratory of Emergency and Trauma, Ministry of Education, College of Emergency and Trauma, Hainan Medical University, Haikou 571199, China.

[f] Jiangsu Key Laboratory of New Drug Research and Clinical Pharmacy, Xuzhou Medical University, Xuzhou, 221004, China.

* Corresponding authors.

E-mail address: leifeng@dmu.edu.cn (L. Feng); tianxiangge1990@163.com (X. Tian); maxc1978@163.com (X. Ma)

‡ These authors contributed equally to this work.

Table of Contents

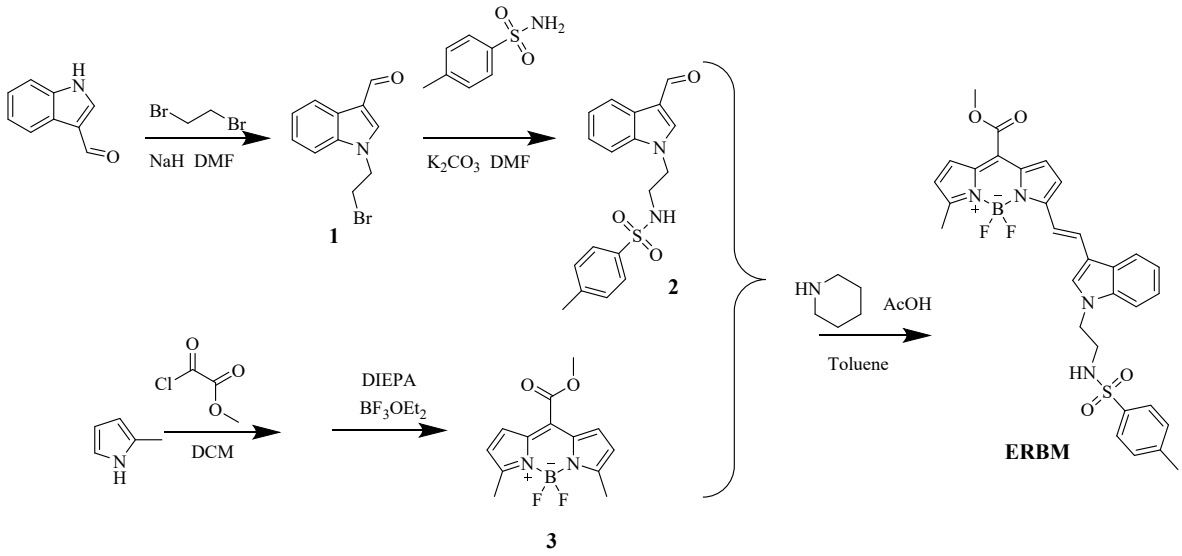

Scheme S1. Synthetic route for **ERBM**.

Synthesis of 1: 480 mg sodium hydride (20 mmol) was added to 20 mL DMF solution containing 1450 mg of 3-indolecarboxaldehyde (10 mmol), then 4 mL 1,2-dichloroethane was added dropwise with stirring at room temperature, increased the temperature to 80 °C and kept stirring for 4 hours. After cooling to room temperature, the reaction solution was added to 200 mL water and extracted three times with 100 mL ethyl acetate. Then ethyl acetate was evaporated under reduced pressure, the residue was further purified by a silica gel column chromatograph using ethyl acetate/petroleum ether (1/2 v/v) as the mobile phase to afford **1** as white solid (1360 mg, yield: 53.9%). ^{1}H NMR (600 MHz, $CDCl_3$) δ 10.03 (s, 1H), 8.35 – 8.31 (m, 1H), 7.79 (s, 1H), 7.40 – 7.31 (m, 3H), 4.60 (t, J = 6.5 Hz, 2H), 3.72 (t, J = 6.5 Hz, 2H).

Synthesis of 2: 750 mg (3 mmol) **1**,770 mg (4.5 mmol) *p*-toluenesulfonamide and 830 mg (6 mmol) potassium carbonate were added to flask, then 30 mL DMF was added with the increasing of temperature to 90 ℃, and kept stirring for 2 hours. After cooling to room temperature, the reaction solution was added to 200 mL water and extracted three times with 100 mL ethyl acetate. Then ethyl acetate was evaporated under reduced pressure, the residue was further purified by a silica gel column chromatograph using ethyl acetate/petroleum ether (1/1 v/v) as the mobile phase to afford **2** as white solid (652 mg, yield: 63.5%). ^{1}H NMR (600 MHz, $CDCl_3$) δ 9.59 (s, 1H), 8.18 – 8.14 (m, 1H), 7.65 – 7.60

(m, 3H), 7.30 – 7.23 (m, 3H), 7.20 (d, J = 8.2 Hz, 2H), 5.78 (t, J = 6.4 Hz, 1H), 4.29 (dd, J = 14.3, 8.4 Hz, 2H), 3.40 – 3.32 (m, 2H), 2.38 (s, 3H). ^{13}C NMR (150 MHz, $CDCl_3$) δ 184.76, 143.85, 139.51, 136.79, 136.53, 129.82, 126.87, 125.33, 124.23, 123.13, 122.32, 118.26, 109.77, 47.45, 42.29, 21.54. HRMS (ESI positive) calcd for $[M+H]^+$ 343.1111, found 343.1108.

3 was synthesized according to this literature [1].

Synthesis of ERBM: 57 mg (0.17 mmol) **2** and 46 mg (0.17 mmol) **3** were added to flask and dissolved with 20 mL toluene. Under N_2 protection, 0.5 mL acetic acid and 0.5 mL piperidine were added to the reaction successively. Then increased temperature to 135 ℃ and kept stirring for 2 hours. After evaporating solution under reduced pressure, the residue was further purified by a silica gel column chromatograph using DCM/MeOH (500/1 v/v) as the mobile phase to afford **ERBM** as blue solid (22 mg, yield: 21.4%). ^{1}H NMR (600 MHz, $CDCl_3$) δ 7.99 (d, J = 7.3 Hz, 1H), 7.62 (td, J = 32.2, 16.1 Hz, 4H), 7.41 – 7.34 (m, 2H), 7.31 – 7.27 (m, 2H), 7.23 (d, J = 8.0 Hz, 2H), 7.17 (d, J = 3.8 Hz, 1H), 6.97 (d, J = 4.7 Hz, 1H), 6.27 (d, J = 4.0 Hz, 1H), 4.78 (t, J = 6.2 Hz, 1H), 4.25 (t, J = 5.8 Hz, 2H), 3.97 (s, 3H), 3.37 (dd, J = 11.8, 6.0 Hz, 2H), 2.66 (s, 3H), 2.39 (s, 3H). ^{13}C NMR (150 MHz, $CDCl_3$) δ 164.86, 159.99, 155.88, 143.95, 137.08, 136.51, 136.46, 133.56, 132.92, 131.85, 131.28, 129.85, 127.76, 126.87, 126.35, 123.59, 122.07, 120.94, 118.82, 117.99, 115.37, 115.30, 109.84, 52.83, 46.87, 42.59, 29.70, 21.52. HRMS (ESI positive) calcd for $[M+H]^+$ 603.2043, found 603.2018.

Experimental section methods

Materials. Various human metabolic enzymes CES1, GLU, Lipase, CES2, α-Glc, β-Glc, β-galactosidase (β-GAL) and HSA were purchased from Sigma Aldrich. Amino acids: serine (Ser), tryptophan (Try), glutamine (Glu), glycine (Gly), arginine (Arg), cysteine (Cys), lysine (Lys), and glutamic acid (Gln) were obtained from Shanghai yuanye. Inhibitors including bis-p-nitrophenyl phosphate, loperamide, ketoconazole, scutellarin, Alogliptin and Irosustat were purchased from Shanghai yuanye. HepG2, LoVo and LO2 cells were obtained from ATCC. ER tracker, Mito tracker and Lys tracker were purchased from Shanghai yisheng. The fluorescence tests were analyzed on a synergy H1 multimode microplate reader (BioTek). HRMS detection was measured on AB Sciex X500R. NMR spectra analysis were acquired in Bruker advance 600.

Synthesis Route for ERBM. The synthesis progresses of these fluorescent candidates are depicted detailly in the supplementary data.

Fluorescence Response of ERBM toward CES1. The activity assay of CES1 was performed in the standard incubation system containing 100 mM potassium phosphate buffer (pH 7.4), CES1 (40 μg/mL) and **ERBM** (10 μM), with a final incubation volume of 200 μL. Then, after incubating at 37 °C for 30 min, 100 μL acetonitrile was added to terminate the reaction and used for microplate reader and HPLC analysis. Next, the standard curve of CES1 enzyme activity was constructed. **ERBM** (10 μM) were incubated with various concentrations of CES1 (0, 1, 2, 3, 5, 10, 20, 30, 40 μg/mL) at 37 ℃ for 30 min, respectively. The detection method was according to the above mentioned.

Selectivity and Stability of ERBM toward CES1. For the selectivity assaying, **ERBM** was incubated separately with different hydrolytic enzymes including CES1, GLU, Lipase, α-Glc, β-Glc, β-GAL, CES2 and HSA. Furthermore, different inhibitors including bis-p-nitrophenyl phosphate (BNPP, CES general inhibitor),[2] loperamide (LPA, CES2 selective inhibitor),[3] ketoconazole (KCZ, general inhibitor for CYP3A),[4] scutellarin (GLU inhibitor),[5] Alogliptin (DPP4 selective inhibitor),[6] and Irosustat (Aryl sulfatase selective inhibitor)[7] were separately incubated with **ERBM** for the chemical inhibition assay.

Additionally, to examine the stability of **ERBM**, the following common metal ions (final concentrations were 10 μM): Mg^{2+}, Ni^{2+}, Ca^{2+}, K^{+}, Mn^{2+}, Zn^{2+}, Sn^{4+}, Cu^{2+}, Ba^{2+}, CO_3^{2-}, SO_4^{2-}, Na^{+} and amino acids (final concentrations were 200 μM): serine (Ser), tryptophan (Try), glutamine (Glu), glycine (Gly), arginine (Arg), cysteine (Cys), lysine (Lys), glutamic acid (Gln) were co-incubated with **ERBM** at 37 °C for 30 min, respectively.

Kinetic Study. To investigate the metabolic characteristics of **ERBM** catalyzed by CES1, the metabolic kinetics was investigated. **ERBM** (0.5 − 200 μM) and CES1 (40 μg/mL) was incubated at 37 °C for 30 min, then the fluorescence intensity versus substrate concentration were fitted into the Eq. 1, and the kinetic parameter K_m was obtained using GraphPad Prism 7.0.

$$V = \frac{V_m * S}{K_m + S} \quad \text{..... Eq.1}$$

Fluorescence Imaging Application and Flow Cytometry Analysis. The fluorescence imaging applications of **ERBM** in live cells was evaluated. HepG2 cells were seeded on

glass polylysine-coated confocal dishes. Next day, **ERBM** was added to the culture cells with the final concentration at 10 μM and incubated at 37 °C for 30 min. Concurrently, BNPP (CES inhibitor, 20 μM) was pretreated for 30 min presenting the inhibition group. After incubation, the cells washed three times to remove the residual **ERBM** and imaged on the confocal microscope (Leica TCS SP8). The imaging condition was as follow: excitation: 633 nm, collection: 650 − 710 nm. Additionally, the application of **ERBM** in flow cytometry analysis was evaluated. LoVo cells and HepG2 cell were collected and incubated with **ERBM** (10 μM) for 10 min and analyzed by flow cytometry.

Subcellular Co-localization. To determine the targeting function of **ERBM** toward ER, co-localization imaging was performed with HepG-2 cells. Briefly, the cells were seeded in 6-wells plate. Next, **ERBM** (20μM) was added into the cell and incubated at 37 ^{o}C for 30 min, Meantime, the organelle tracker including: ER tracker Green BODIPY® FL Glibenclamide, (0.1μM), LysoTracker Green DND-26 (0.2μM), and MitoTracker® Green FM (0.2μM) were added respectively[8]. Then, the cells were washed and imaged on the Leica TCS SP8.

CES1 Activity Evaluation under ER Stress. ER stress is an autoregulatory response of cells in a variety of disease states.[9] **ERBM** was used to detect the changing pattern of CES1 under ER stress. DTT (4 mm), a model drug inducing ER Stress, was added into LO2 cells and co-incubated 12 h, the control group was set without DTT. After then, replace the original culture medium with fresh culture medium containing **ERBM**, incubated at 37 ^{o}C for 30 min, and imaged as mentioned above. Meanwhile, the protein changes of CES1 were also analyzed by Western Blot.

Regulation of CES1 in LO2 Cells for Liver Injury. APAP (4 mM), the classical acute liver injury drug,[34] was added into LO2 cells and incubated for 48 h, and the control group was set without APAP. Then, **ERBM** was added into the cells and incubated for 30 min. At last, the cells were imaged on Leica TCS SP8.

In Vivo Imaging of CES1. In this paper, the endogenous of CES1 in mice was imaged by **ERBM**. The imaging conditions were excitation wavelength 605 nm, fluorescence acquisition band 700 ± 20 nm. **ERBM** was administered by tail vein injection at a concentration of 20 μM. After the administration, the fluorescence imaging was collected within 0 − 1 h. At the same time, the inhibitor group was set by pretreating with BNPP (20

μM). All the animals' experiments were according to the guidelines approved by the ethics committee of Dalian Medical University and the case number was AEE19047. Additionally, the organs liver, heart, kidney, lung, spleen, and intestine were dissected from the mice, and incubated with **ERBM** at 37 ℃ for 30 min, then fluorescence imaging for the expression in different organs were imaged.

Activity Changes of CES1 in APAP-Induced Acute Liver Injury. Acute liver injury is often accompanied by a significant ER stress response, herein, an acute liver injury model was established using APAP to explore the regulation characteristics of CES1 under ER stress. C57BL/6J mice were divided into control (saline) and APAP groups (n = 6 in each group); the dose of APAP was set at 400 mg/kg for 12 hours. At last, liver tissues were collected for H&E staining analysis. Meanwhile, a portion of the liver was harvested for frozen section and stained with **ERBM** foe fluorescence imaging. Furthermore, the changes of CES1 were also evaluated by Western Blot.

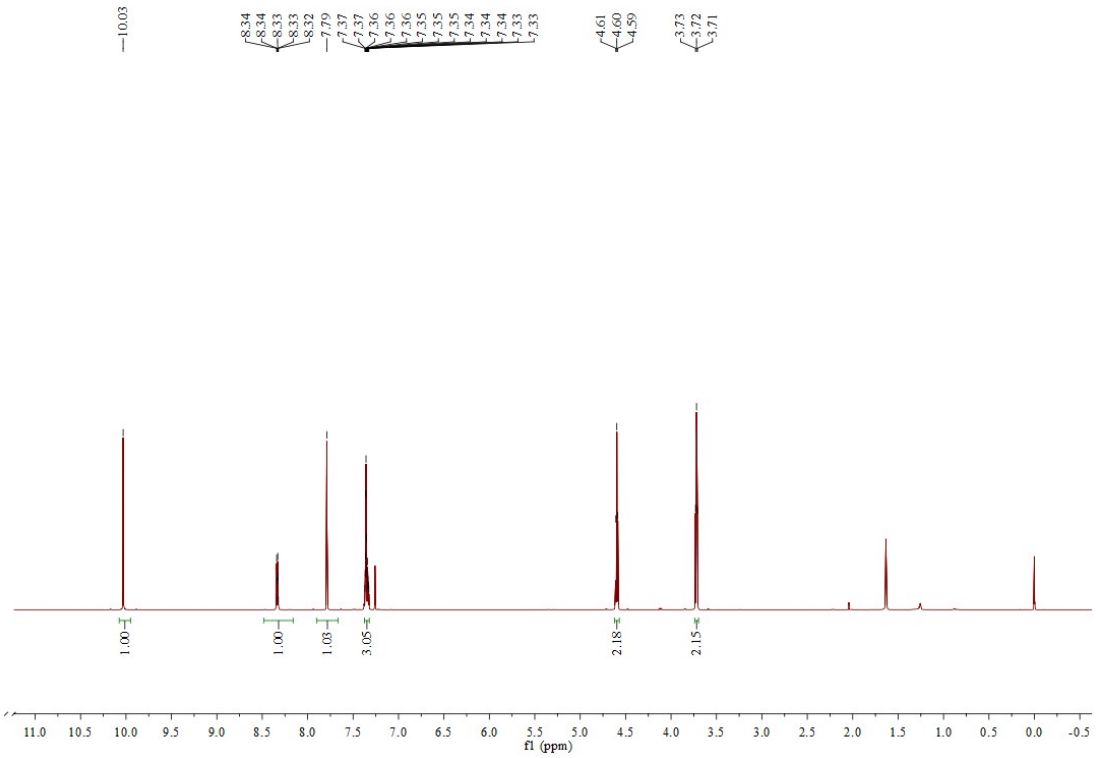

Figure S1. ^{1}H NMR spectrum of **1** in $CDCl_3$.

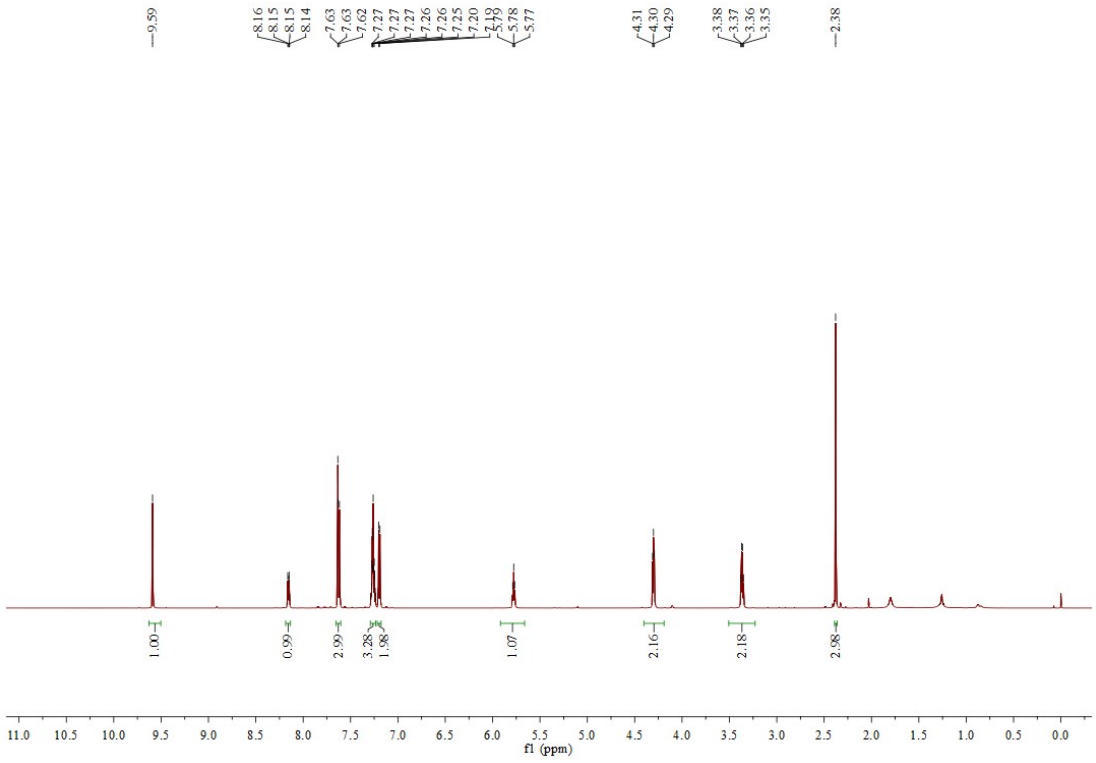

Figure S2. ^{1}H NMR spectrum of **2** in $CDCl_3$.

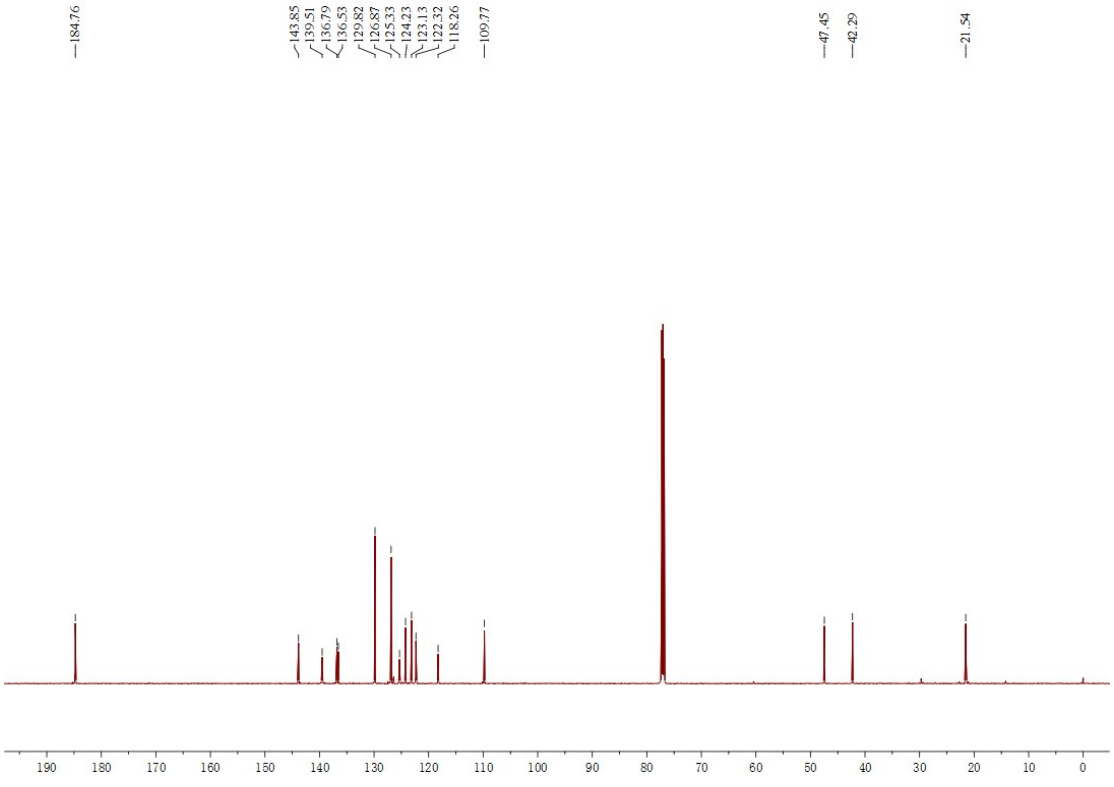

Figure S3. ^{13}C NMR spectrum of **2** in $CDCl_3$.

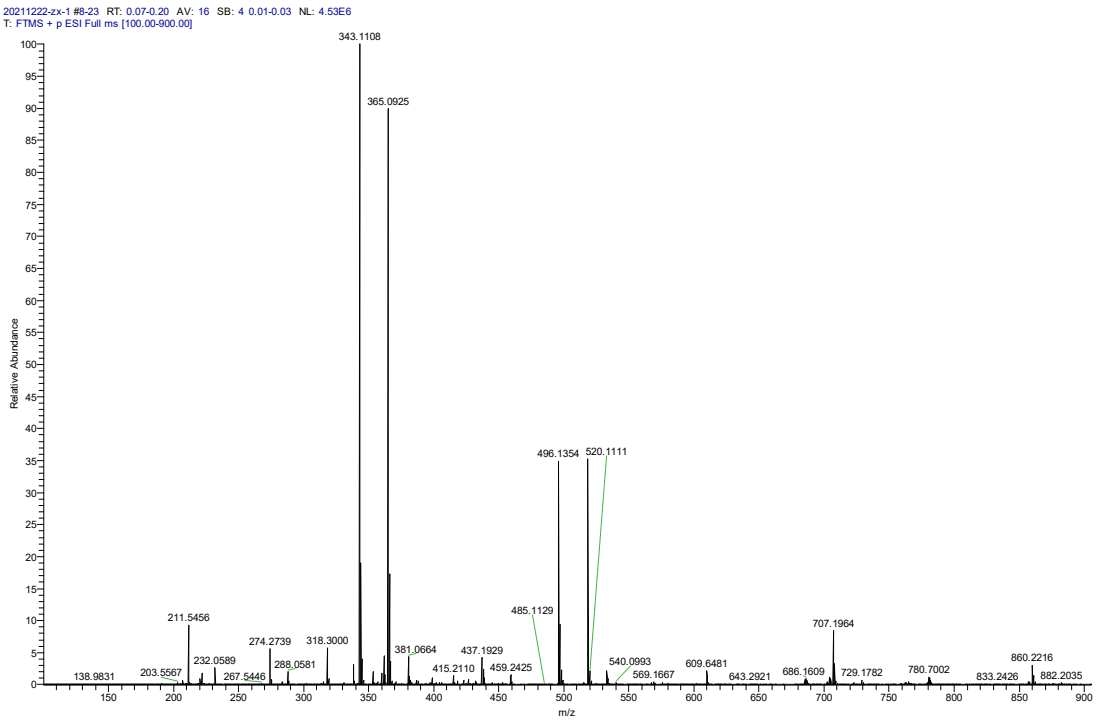

Figure S4. HRMS of **2**.

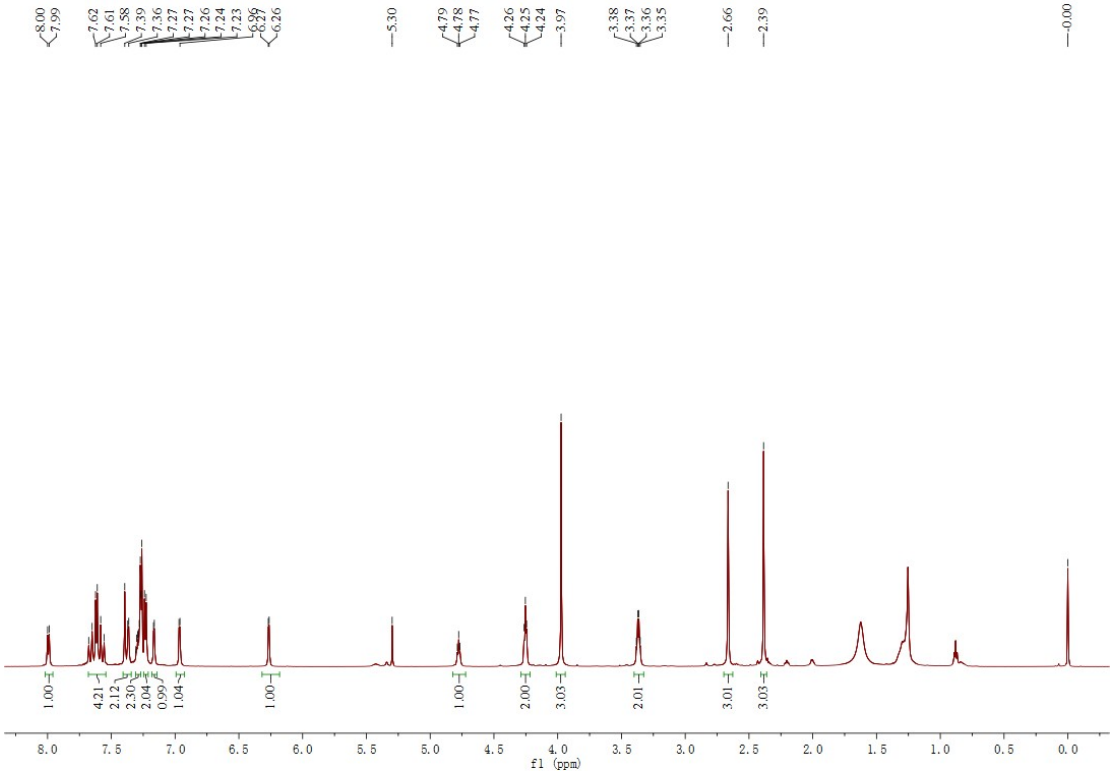

Figure S5. ^{1}H NMR spectrum of **ERBM** in $CDCl_3$

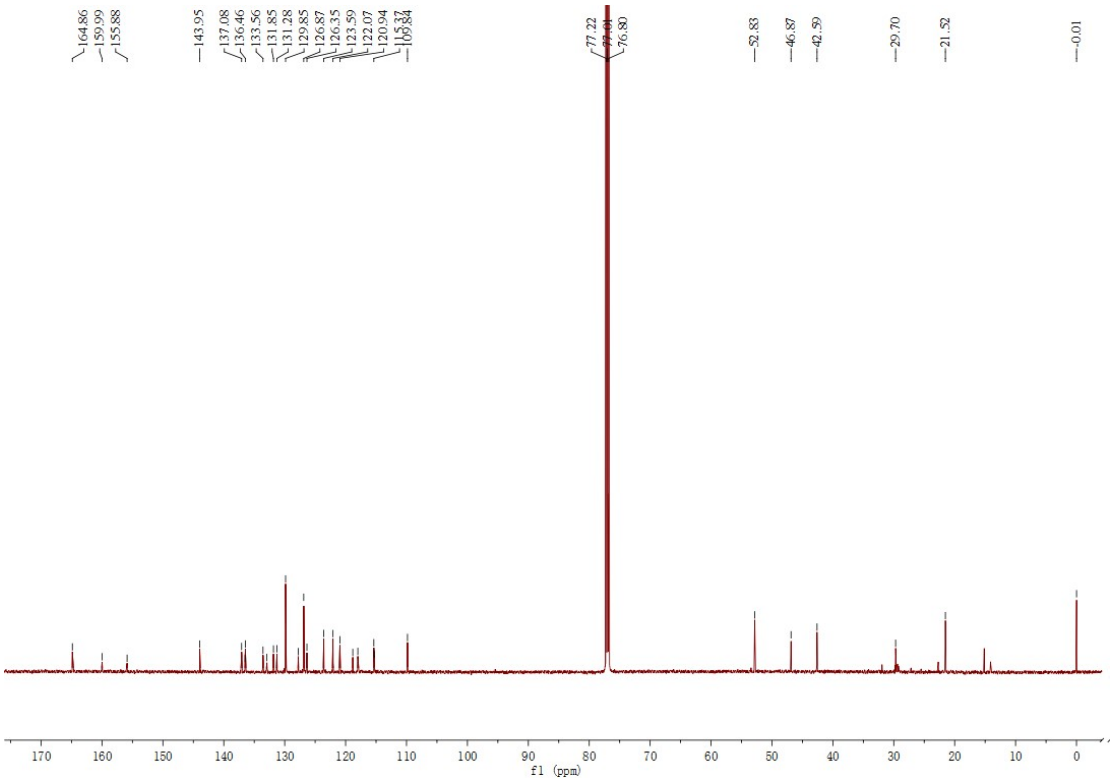

Figure S6. ^{13}C NMR spectrum of **ERBM** in $CDCl_3$

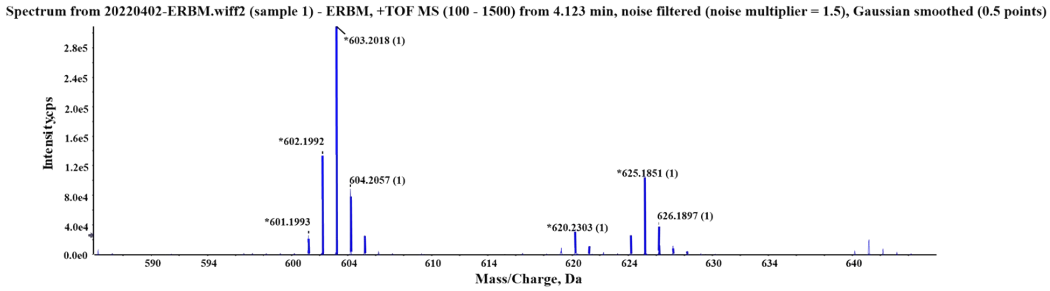

Figure S7. HRMS of **ERBM**.

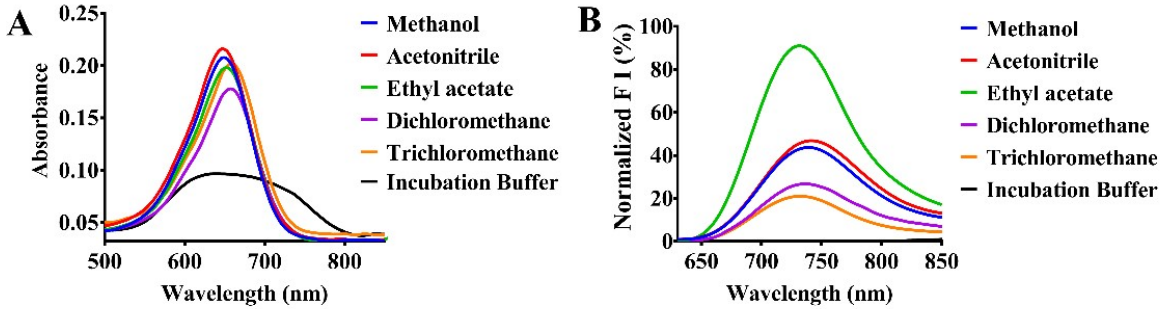

Figure S8 Absorption (A) and fluorescence (B) spectra of ERBM indifferent solvents.

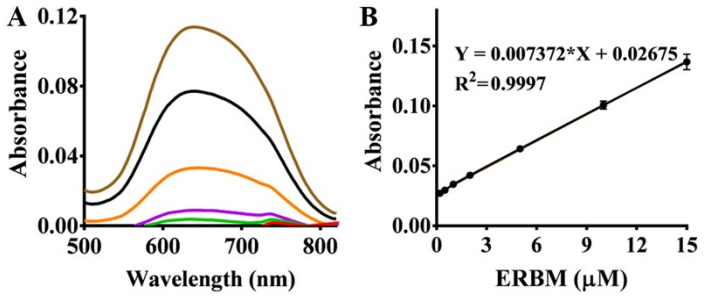

Figure S9 Absorption spectra (A) and the linear regression (B) of OD values at 660 nm toward different concentrations of **ERBM** (0.2 – 15 μM) in 100 mM potassium phosphate buffer (pH 7.4).

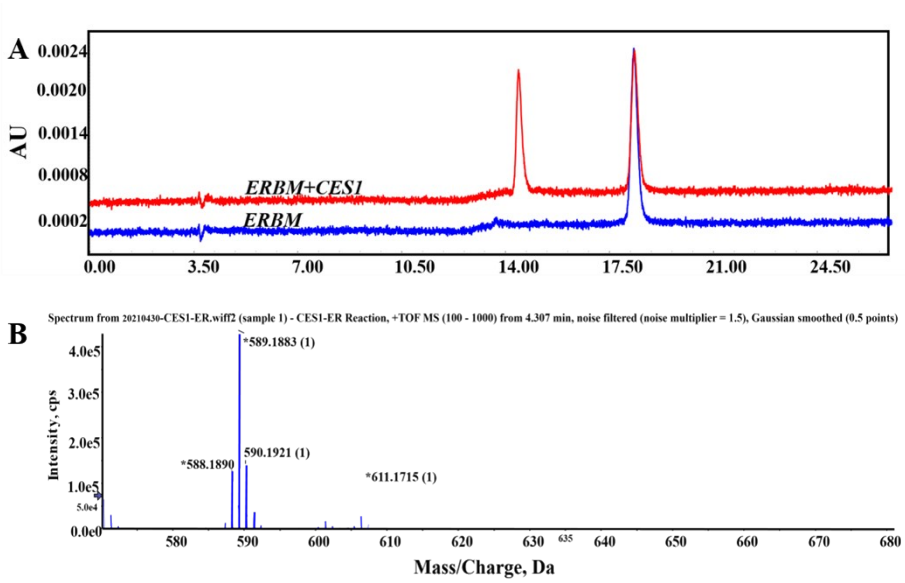

Figure S10 (A) HPLC chromatogram of the **ERBM** standard (Blue) and incubation sample (Red); (B) HRMS of the product after bio-transformed by CES1.

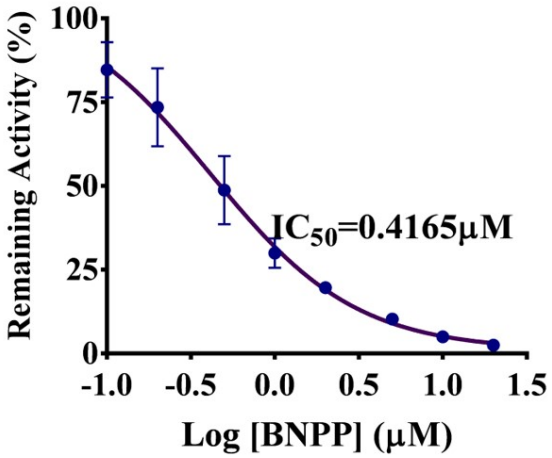

Figure S11 The inhibition IC_{50} curve of BNPP toward CES1.

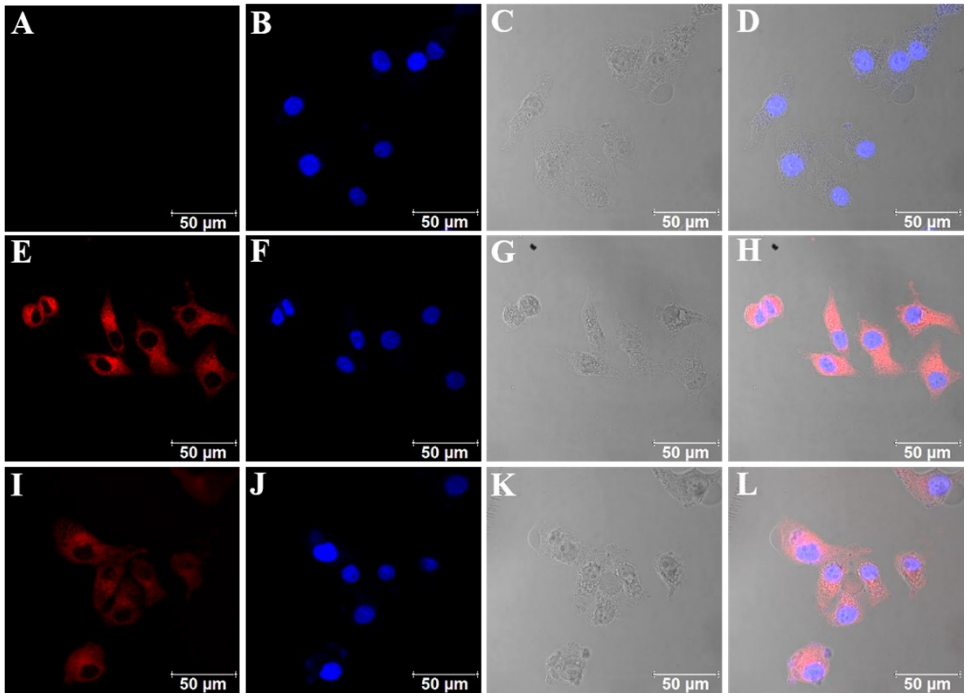

Figure S12. Fluorescence imaging of endogenous CES1 in HepG2 cells. (A, E, I) Fluorescence field; (B, F, J) Nucleus location stained by Hoechst 33342; (C, G, K) Bright field; (D, H, L) Overlapping images. The excitation wavelength was 633 nm, and the fluorescence signals were collected from 650 − 710 nm, scale bar 50 μm.

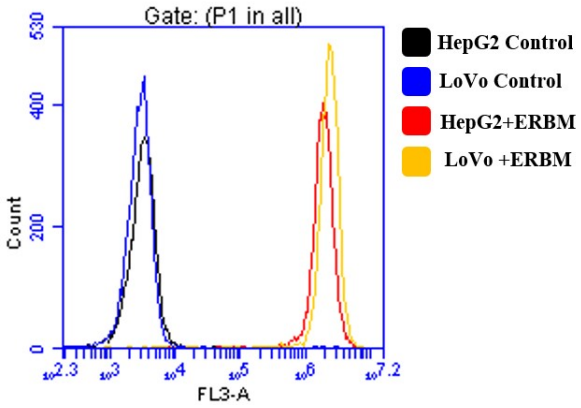

Figure S13 Flow cytometry analysis in HepG2 cells and LoVo cells.

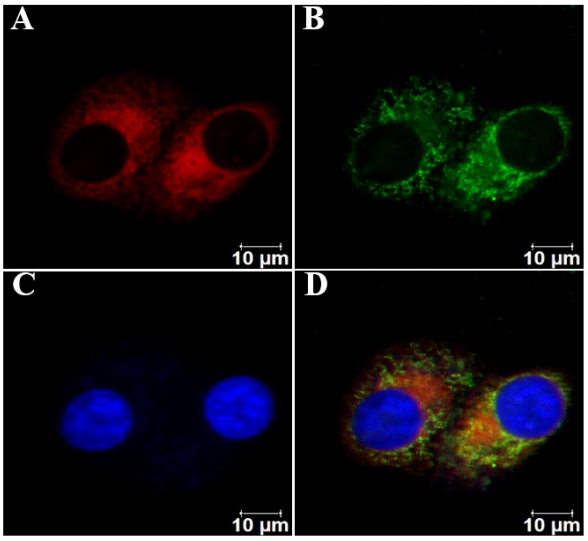

Figure S14. Colocalization between **ERBM** and Mito-Tracker (Green). (A) Fluorescence images of ERBM (650 − 710 nm); (B) Fluorescence signal imaging of Mito-Tracker (535 − 585 nm); (C) Nucleus location stained by Hoechst 33342; (D) Merged fluorescence image.

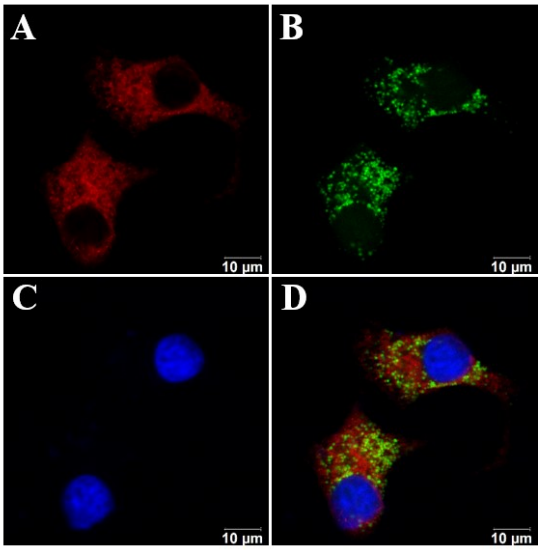

Figure S15. Colocalization between **ERBM** and Lys-Tracker (Green). (A) Fluorescence images of **ERBM** (650 − 710 nm); (B) Fluorescence signal imaging of Lys-Tracker (535 – 585) nm; (C) Nucleus location stained by Hoechst 33342; (D) Merged fluorescence image.

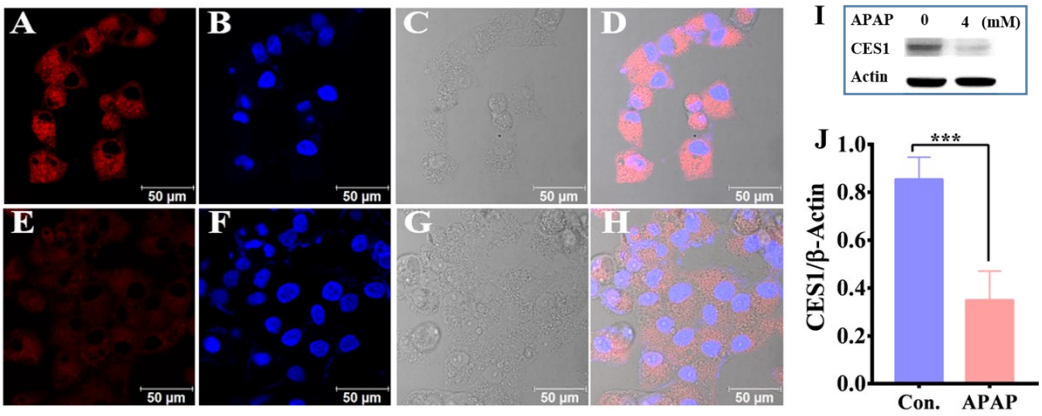

Figure S16. Fluorescence imaging of the regulation of CES1 under the APAP-induced liver injury model in LO2 cells. (A) Fluorescence imaging after incubating with ERBM; (E) fluorescence imaging after treatment with APAP; (B, F) Nucleus staining; (C, G) bright field; (D, H) merged of all channels; (I, J) the image and gray analysis of Western Blot. Scale bar 50 μm.

REFERENCES

[1] Z. H. Tian, L. L. Ding, K. Li, Y. Q. Song, T. Y. Dou, J. Hou, X. G. Tian, L. Feng, G. B. Ge and J. N. Cui, *Analytical Chemistry* **2019**, *91*, 5638-5645.

[2] a) D. D. Wang, L. W. Zou, Q. Jin, J. Hou, G. B. Ge and L. Yang, *Acta Pharmaceutica Sinica B* **2018**, *8*, 699-712; b) W. Lei, D. D. Wang, T. Y. Dou, J. E. Hou, L. Feng, H. Yin, Q. Luo, J. E. Sun, G. B. Ge and L. Yang, *Toxicology And Applied Pharmacology* **2017**, *321*, 48-56.

[3] a) Y. N. Lin, M. Jiang, W. J. Chen, T. J. Zhao and Y. F. Wei, *Biomedicine & Pharmacotherapy* **2019**, *118*; b) M. Bhardwaj, N. M. Leli, C. Koumenis and R. K. Amaravadi, *Seminars In Cancer Biology* **2020**, *66*, 116-128.

[4] B. B. Chen, J. H. Yan, J. Zheng, H. W. Peng, X. L. Cai, X. T. Pan, H. Q. Li, Q. Z. Hong and X. E. Peng, *Scientific Reports* **2021**, *11*.

[5] R. J. Fontana, *Gastroenterology* **2014**, *146*, 914-U437.

[6] M. Gabriele, P. Puccini, M. Lucchi, A. Vizziello, P. G. Gervasi and V. Longo, *Biochemical Pharmacology* **2018**, *150*, 64-71.

[7] M. Taketani, M. Shii, K. Ohura, S. Ninomiya and T. Imai, *Life Sciences* **2007**, *81*, 924-932.

[8] X. Y. Xiang, X. C. Yang, J. Su, J. S. Kang, Y. Wu, Y. N. Xue, Y. T. Dong and L. K. Sun, *Oncology Reports* **2016**, *35*, 3471-3479.

[9] H. O. Rashid, R. K. Yadav, H. R. Kim and H. J. Chae, *Autophagy* **2015**, *11*, 1956-1977.